

# Turbulent Momentum Interchange Between Connected Flow Passages

J.D. HOOPER

Research Scientist, Engineering Research Division, Australian Atomic Energy Commission

and

W.J. CRAWFORD and M.J. HINCKSMAN

Technical Officers, Australian Atomic Energy Commission

## 1 INTRODUCTION

The turbulent interchange of heat, mass and momentum between parallel flow channels, interconnected by a continuous and narrow gap, is an interesting aspect of many engineering applications of fluid mechanics. Specifically, in nuclear power reactor cores, formed by large symmetrical arrays of parallel cylindrical fuel pins and spaced at low ( $p/d$ ) ratios, the interchange of fluid in the rod gap region has been extensively studied. Most of this work has concentrated on the use of an inert tracer, such as nitrous oxide in air, or salt in water, to measure the mass transfer between adjacent flow areas or subchannels. Such measurements are expressed as a gross diffusion coefficient, which is specific to the experimentally simulated rod bundle geometry. In addition, such factors as the range of Reynolds numbers tested, entry conditions, and the presence or absence of turbulence promoters such as spacer grids in the array influence the magnitude of such coefficients. Although, by evaluating it as a gradient diffusion process ignores the transport mechanism of turbulence created by secondary flows, it is of direct use to the sub-channel analysis codes used in reactor core analysis (Rowe 1973a).

The most significant finding of the experiments based on the above method was that the gross inter-subchannel mass transfer rates were insensitive to the actual gap width, and their approximate constancy over a large range of rod ( $p/d$ ) ratios. Galbraith and Knudsen (1972) employed a square pitch rod array in the ( $p/d$ ) ratio range of 1.011 to 1.228 to illustrate this effect. If turbulent diffusion were the sole mechanism of transfer, the gross transfer rates would be determined by the gap width. It was concluded that additional fluid processes affect the transfer rates, the most probable being secondary flows.

In addition to the gross mixing experiments, there has been recently a significant effort in detailed fine scale measurement of the mean flow parameters (mean axial velocity and wall shear stress) together with some of the six turbulent Reynolds stress terms for developed single phase turbulent rod bundle flow. Rowe (1973b) and Rehme (1978) used a square pitched rod array for their experiments, whereas Kjellström (1974), Trupp and Azad (1975), Carajilescov and Todreas (1975), and Vonka and Hoornstra (1979) used either a triangular pitch or a mixed rod bundle. Despite the use of laser-Doppler anemometry in several of these studies, the presence of secondary flows was not established conclusively.

## 2 EXPERIMENTAL RIG

The limited published data on turbulence intensity for rod bundle flows, together with the increased use of numerical turbulence modelling, were the two factors that initiated the development of the six-rod cluster air rig at the AAEC Research Establishment. The test section cross-section is shown in Figure 1, with two subchannels of a square pitch rod array being modelled. The effect of the presence of the gap walls in all rod gap regions other than the central interconnected region has been numerically shown, for laminar flow conditions, to be negligible in this region for the two ( $p/d$ ) ratios studied, 1.194 and 1.107 (Hooper 1977).

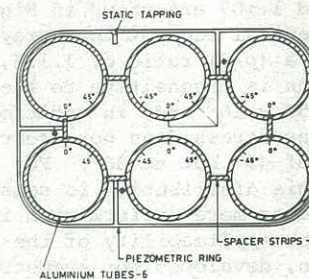


Figure 1 Rig cross-section

The rod diameter was 14 cm and the length of the test section was 9.14 m. The axial static pressure gradient was determined by 19 static tap locations equally spaced along the test section; a settling drum of diameter 1.2 m having an internal fine-mesh screen was used before the flow entry to the test section. The air rig was powered by either a 45 kW or a 26 kW centrifugal blower, connected to the settling drum by approximately 10 m of 20 cm dia - meter pipe.

All reported measurements were made at an axial plane 10 cm from the rig exit, and the mean velocity parameters were wall shear stress and mean axial velocity, measured respectively by Preston tubes and Pitot probes.

The measurement of the six turbulent Reynolds stress terms, even for the symmetry zone shown by Figure 1, required hundreds of hours of experimental work. The rig probe transport and rotation system, together with hot-wire rotation, signal line switching and signal gain control was completely automated, and the rig was run overnight under the control of the Noise Analysis Laboratory PDP 11/10 computer.

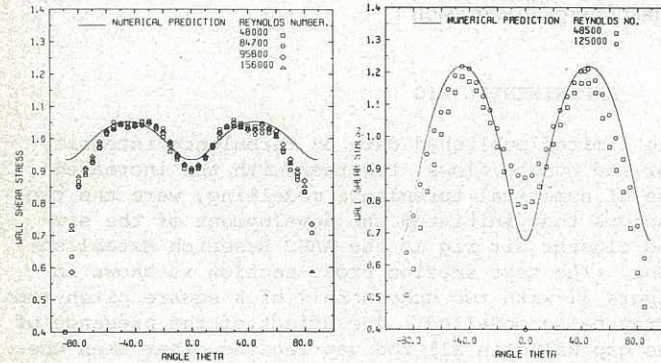
The hot-wire probes comprised a single straight wire and single inclined wire, each made from copper plated 5  $\mu$ m tungsten wire with an active length of 2 mm. The probe production techniques and response correlations were those developed by workers at the



I.S.V.R., Southampton (Bruun 1971). Hot wires were used primarily to measure the turbulence intensities, and a computer stored mean radial velocity profile, appropriately scaled for the day conditions to maintain a constant rig  $Re$ , was used to calibrate the probe during each traverse and calculate the Reynolds stress terms. The unlinearised signal output, similar to that used by Perry and Abell (1975) for developed pipe flow measurements, was employed.

### 3 MEAN FLOW RESULTS

The wall shear stress distributions for the (p/d)



(a)  $p/d = 1.194$  (b)  $p/d = 1.107$

Figure 2 Wall shear stress distribution

ratios, 1.194, and 1.107 are shown in Figures 2(a) and (b) for the central rods of the array. It is apparent that for a (p/d) ratio of 1.194, the shear stress distribution is insensitive to the  $Re$  over the range  $48$  to  $150 \times 10^3$  and, in addition, that the peak wall shear stress does not occur at the axis of symmetry of  $45^\circ$  but at  $30^\circ$ . For the (p/d) ratio of 1.107, this distribution is sensitive to the flow  $Re$ , becoming more uniform with increasing mean velocity. The applicability of the Patel (1965) correlation, developed for symmetrical pipe flow, was tested at several azimuthal angles for the (p/d) of 1.194, using 12 Preston tubes ranging from 0.056 cm to 0.400 cm o.d. The results were consistent within the accuracy of measurement for the three regions of the correlation, i.e. the viscous sublayer, transition region and turbulent core. However, an increasing trend in the calculated shear was noted for a (p/d) ratio of 1.107, using two tubes of 0.127 and 0.2032 cm diameter, in a ratio of 0.983:1.0. This is probably due to the gross departure of the flow structure from axisymmetric pipe flow, as the probe wall distance increased for this rod spacing.

The mean velocity profiles scaled by the local wall friction velocity are shown in Figures 3(a) and (b) for a (p/d) of 1.107. The profiles in the gap region give a flatter distribution than the law of

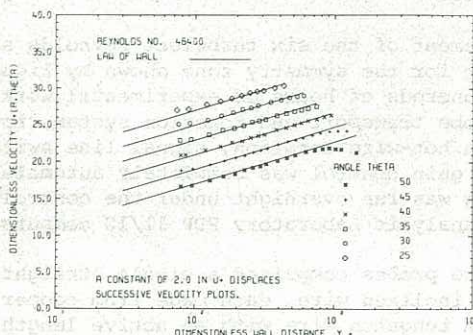


Figure 3(a) Radial velocity profile  $p/d = 1.107$

the wall, using the constants 0.40 for the von Karman constant and 5.5 for  $C$ . For a (p/d) of 1.194, the profiles are well scaled by the law of the wall for all azimuthal angles, but the distributions are not shown.

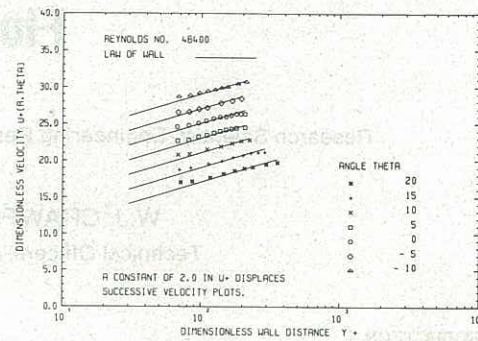


Figure 3(b)

### 4 TURBULENCE INTENSITIES

The turbulence intensities, normalised by the local wall shear stress, for a (p/d) of 1.194 and  $Re$  of  $48 \times 10^3$  and a (p/d) of 1.107 and  $Re$  of  $48.4 \times 10^3$  are shown in Figures 4(a) to (e) and 5(a) to (e).

#### 4.1 Axial Intensity $u'$

The axial intensity for a (p/d) of 1.194 and a  $Re$  of  $48 \times 10^3$  is shown by Figure 4(a). The intensity along the  $\theta = 45^\circ$  symmetry line scales closely to the data reported for developed pipe flow (Laufer 1954, Lawn 1971). As the rod gap is approached, the axial intensity becomes increasingly large at the centre-line.

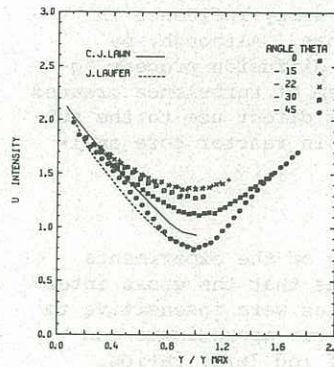


Figure 4(a)

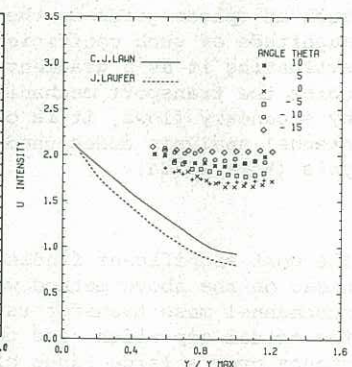


Figure 5(a)

Axial intensity  $u'$

For the (p/d) of 1.107, the  $\theta = 45^\circ$  traverse also approximated to developed pipe flow. However, in the gap region (Figure 5(a)) for a range of azimuthal angles from  $\theta = 0$  to  $\pm 15^\circ$  the distribution is essentially flat and independent of wall distance. This is in agreement with the results of Rowe (1973b), who used a laser-Doppler system in a square pitch array at a (p/d) of 1.125 and water as the working fluid. Unfortunately, his results did not include any of the other stress terms. Other workers, mentioned above, either used a triangular pitch array or mixed geometry test section with (p/d) ratios greater than 1.20. Numerical studies have shown that the azimuthal wall shear stress variation is significantly smaller for a triangular array than the square pitched array at the same (p/d) ratio. As the change in flow structure from the axisymmetrical pipe distribution is closely related to the azimuthal variation of the wall shear stress, the studies of Kjellström (1974), Trupp and Azad (1975), and Carajilescov and Todreas (1975), in which the wall shear stress variation was less than



4%, showed turbulence intensities very similar to the reported values for developed pipe flow at all azimuthal angles.

#### 4.2 Radial Intensity $v'$

The radial intensity at  $\theta = 45^\circ$  again approximated the pipe distributions. As the gap region was approached, the degree of departure from the axisymmetric distribution became more marked, particularly for the lower (p/d) ratio of 1.107 (Figures 4(b) and 4(c)).

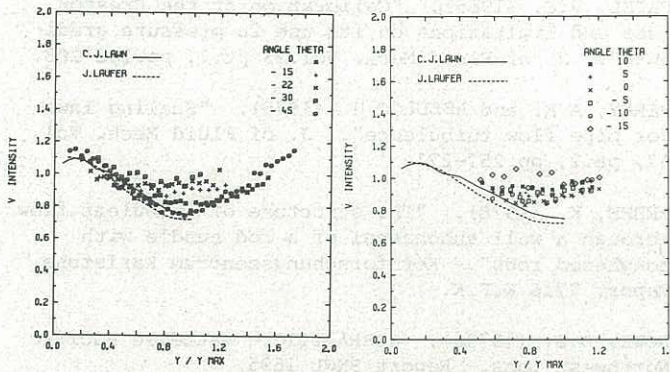


Figure 4(b)

Figure 5(b)

Radial intensity  $v'$

#### 4.3 Azimuthal Intensity $w'$

From Figures 4(c) and 5(c), it can be seen that the azimuthal turbulence intensity has a curve similar to those of the other two normal components. The departure from the pipe distributions is most marked in the rod gap region for a (p/d) ratio of 1.107, where the azimuthal intensity is almost uniform and considerably higher than the pipe distribution. The closest wall distance possible with the rotated hot wire probe was 0.45 cm, a distance which could not be reduced by the use of more closely spaced probe support forks. This is partly because of the need to have at least 1.5 mm of plated wire separating the active length of the probe from the forks to minimise probe support interference.

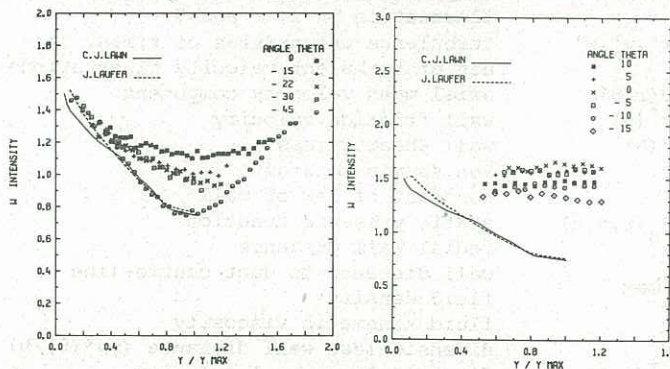


Figure 4(c)

Figure 5(c)

Azimuthal intensity

#### 4.4 Radial Turbulent Shear Stress $-\rho \overline{uv}$

The radial turbulent shear stress is shown in Figures 4(d) and 5(d). For a (p/d) ratio of 1.194, this component along the  $\theta = 0$  (rod gap) traverse asymptotes to the local wall shear stress value, in common with developed pipe flow. In the rod gap region, at  $\theta = 0$ , for a (p/d) ratio of 1.107 the same result is obtained. However, at  $45^\circ$  and with the smaller (p/d) ratio, a significant curvature is seen in the shear stress distribution.

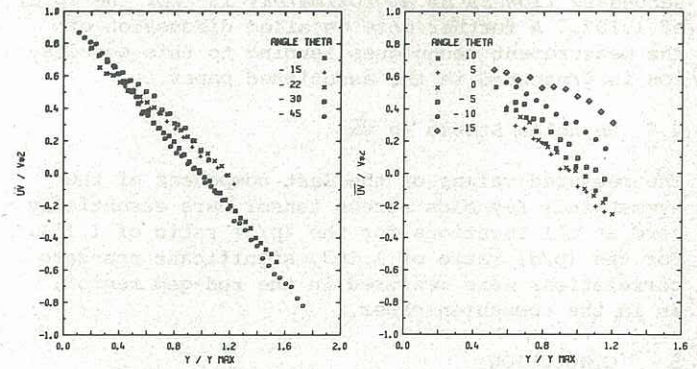


Figure 4(d)

Figure 5(d)

Radial turbulent shear  $-\rho \overline{uv}$

It is proposed that this curvature is associated with a fundamental change in the secondary flow pattern in the rod gap region, from a basic single cell loop at a (p/d) of 1.194 to a two-cell structure for a (p/d) of 1.107. The presence of a linear stress gradient in the gap region lends support to the existence of a static pressure field of the form,

$$P_s(z, r, \theta) = kz + \phi(r, \theta) \quad (1)$$

for the developed flow region, where  $k$  is the constant axial pressure gradient. This proposition is examined at greater length in a companion paper (Hooper 1980).

#### 4.5 Azimuthal Turbulent Shear Stress $-\rho \overline{uw}$

The azimuthal shear stress distribution for the (p/d) ratio of 1.194 is shown in Figure 4(e) and, as required by symmetry, this component is essentially zero at  $\theta = 0$  and  $45^\circ$ . The other azimuthal angles show no great changes in this distribution, although the correlation  $uw$  is far from zero within the symmetrical flow area.

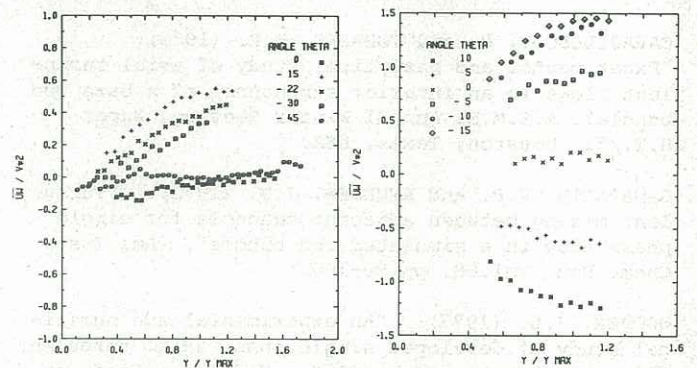


Figure 4(e)

Figure 5(e)

Azimuthal turbulent shear  $-\rho \overline{uw}$

For a (p/d) of 1.107 (Figure 5(e)), a transformation occurs in the  $-\rho \overline{uw}$  distribution. From a value of zero at  $\theta = 0$ , this component increases to approximately 1.5 times the local wall shear stress, at an angle of  $15^\circ$ . This behaviour is symmetrical across the rod gap and with respect to the top and lower centre line rods, and gives a strong indication of a fundamental change in the turbulent flow structure for the two different (p/d) ratios in the rod gap region. Essentially, the single circulation loop of secondary flow has transformed into a two-loop counter-rotating system and, in place of the four cells bounded by  $\pm 45^\circ$  for the top and bottom centre-line rods at a (p/d) of 1.194, there are now eight. The node in the azimuthal component of



secondary flow is at approximately  $15^\circ$  for the (p/d) of 1.107. A further more detailed discussion of the measurement techniques leading to this conclusion is presented in the associated paper.

#### 4.6 Reynolds Stress $-\rho \overline{vw}$

The measured values of the last component of the symmetrical Reynolds stress tensor were essentially zero at all locations for the (p/d) ratio of 1.194. For the (p/d) ratio of 1.107, significant non-zero correlations were measured in the rod-gap region, as in the companion paper.

### 5 CONCLUSION

The turbulent flow structure in closely spaced rod bundle geometry, for the developed flow region, departs markedly from the accepted distributions of axisymmetric pipe flow. This departure is associated with the presence of secondary flow cells which circulate in symmetrical zones of the cluster, and which act to equalise the wall shear stress distribution. The structure of the secondary flow changes as the rod spacing decreases from a one-cell system at a (p/d) ratio of 1.194 to a two-cell system at a (p/d) of 1.107. This effect is most clearly shown by the change in the azimuthal component of the Reynolds stress tensor in the rod gap region, and by the presence of a significant correlation between the two non-axial components of turbulent velocity,  $-\rho \overline{vw}$ , in this region. The fluid transport by secondary flow is apparently the mechanism which maintains the mixing rates of an inert tracer substance across the rod gap region, substantially independent of the gap width, an effect noted in many earlier mixing experiments in rod bundle geometry.

### REFERENCES

BRUUN, H.H. (1971). "Interpretation of a hot wire signal using a universal calibration signal". J. of Phys. E. Sci. Inst. Vol.4, pp.225-31.

CARAJILESCOV, P. and TODREAS, N.E. (1975). "Experimental and analytical study of axial turbulent flows in an interior subchannel of a bare rod bundle". A.S.M.E. Annual Winter Meeting, Paper H.T./51, Houston, Texas, USA.

GALBRAITH, K.P. and KNUDSEN, J.G. (1972). "Turbulent mixing between adjacent channels for single phase flow in a simulated rod bundle". Am. Inst. Chem. Eng. Vol.68, pp.90-100.

HOOVER, J.D. (1977). "An experimental and numerical study of developed single phase axial turbulent flow in a smooth rod bundle". 2nd Aust. Conf. on Heat and Mass Transfer, Sydney, February, 1977, pp.241-248.

HOOVER, J.D. (1980). "Measurement of secondary flows in rod bundle duct flow". Paper 7th Aust. Hyd. & Fluid Mech. Conf.

KJELLSTRÖM, B. (1974). "Studies of turbulent flow parallel to a rod bundle of triangular array". Aktiebolaget Atomenergi Studsvik, Nyköping, Sweden, Report AE-487.

LAUFER, J. (1954). "The structure of turbulence in fully developed pipe flow". N.A.C.A. Report 1174.

LAWN, C.J. (1971). "The Determination of the rate of dissipation in turbulent pipe flow". J. of Fluid Mech., Vol.48, pt.3, pp.477-505.

PATEL, V.C. (1965). "Calibration of the Preston tube and limitations on its use in pressure gradients". J. of Fluid Mech. Vol.23 pt.1, pp.185-208.

PERRY, A.E. and ABELL, C.J. (1975). "Scaling laws for pipe flow turbulence". J. of Fluid Mech. Vol. 67, pt.2, pp.257-271.

REHME, K. (1978). "The structure of turbulent flow through a wall subchannel of a rod bundle with roughened rods". Kernforschungszentrum Karlsruhe, Report 2716 K.F.K.

ROWE, D.S. (1973a). COBRA IIIC. Battelle Pacific Northwest Labs. Report BNWL 1695.

ROWE, D.S. (1973b). "Measurement of turbulent velocity, intensity and scale in rod bundle flow channels". Battelle Pacific Northwest Labs. Report BNWL 1736.

TRUPP, A.C. and AZAD, R.S. (1975). "The structure of turbulent flow in triangular array rod bundles". Nuc. Eng. & Design, Vol.32, pp.47-84.

VONKA, V. and HOORNSTRA, J. (1979). "A hydraulic experiment to support calculations of heat mixing between reactor subchannels". Conf. Paper, 2nd Symposium on Turbulent Shear Flows, London, July.

### NOTATION

p/d	rod pitch to diameter ratio
Re	Reynolds number ( $\bar{U} d_h / \nu$ )
u, v, w	instantaneous values of velocity
	fluctuation in z, r and $\theta$
u', v', w'	turbulence intensities or r.m.s. values of turbulent velocity fluctuations
U(r, $\theta$ )	axial mean velocity component
$v^*(\theta)$	wall friction velocity
$\tau(\theta)$	wall shear stress
K	Von Karman constant
C	constant of law of wall
$P_s(r, \theta, z)$	static pressure function
$y_s$	radial wall distance
$y_{max}$	wall distance to duct centre-line
$\rho$	fluid density
$\nu$	fluid kinematic viscosity
$y^+$	dimensionless wall distance ( $y v^*(\theta) / \nu$ )
$U^+(r, \theta)$	dimensionless axial velocity ( $U(r, \theta) / v^*(\theta)$ )
$\bar{U}$	Average velocity 0 to $45^\circ$ segment
$d_h$	duct hydraulic diameter